PHILOSOPHICAL TRANSACTIONS OF THE ROYAL SOCIETY A MATHEMATICAL, PHYSICAL & ENGINEERING SCIENCES

The Energy Balance and Deformation Mechanisms of Thrust Sheets

D. Elliott

Phil. Trans. R. Soc. Lond. A 1976 **283**, 289-312
doi: 10.1098/rsta.1976.0086

Phil. Trans. R. Soc. Lond. A. **283**, 289–312 (1976) [289]
Printed in Great Britain

The energy balance and deformation mechanisms of thrust sheets

By D. Elliott
Department Earth and Planetary Sciences, The Johns Hopkins University, Baltimore, Maryland 21218, *U.S.A.*

[Plates 12 and 13]

The total energy involved in emplacing a thrust sheet is expended in initiation and growth of the thrust surface, slip along this surface, and deformation within the main mass of the sheet. This total energy can be determined from potential energy considerations knowing the initial and final geometry from balanced cross sections after defining the thrust's thermodynamic system boundaries. Emplacement of the McConnell thrust in the Canadian Rockies involved *ca.* 10^{19} J of gravitational work, an order of magnitude greater than any possible work by longitudinal compressive surface forces. A new theory for the initiation and growth of thrusts as ductile fractures is based on a demonstration that thrust displacement is linearly related to thrust map length and that fold complexes at the ends of thrusts are constant in size for a given metamorphic grade. Much of the total work is dissipated within the body of the sheet. Field observations show which mechanisms of dissipation are most important at various positions within the thrust sheet, and it is found that only the top 5 km of the McConnell was dominated by frictional sliding. A novel type of sliding along discrete surfaces is pressure solution slip, in which obstacles are by-passed by diffusive mass transfer. Fibres and pressure solution grooves are diagnostic features of this sliding law, in which slip velocity is linearly related to shear stress. Pressure solution slip is widespread at depths greater than about 5 km, but at this depth penetrative whole rock deformation by pressure solution becomes dominant – marked by cleavage and stretching directions – and accounts for much of the finite strain within the thrust sheet. The McConnell thrust has an outer layer which deformed by frictional sliding and this overlies a massive linearly viscous core responsible for much of the energy dissipation and gross mechanical behaviour.

Symbols

a, b thickness and length of ductile zone at end of thrust
A amplitude of sinusoidal surface
C, C', K, K' dimensionless constants
d diameter of perfectly plastic zone at tip of ductile crack and also used for mean diameter of grains
D diffusion coefficient
g gravitational acceleration
h, $\bar{h}$ thickness of thrust sheet and mean thickness averaged over dip length p
H, H_j, H_0, H', ΔH centre of gravity in general, of volume element, of original state, of final state, and change in centre of gravity of thrust sheet
k Boltzmann constant
l, p strike length measured on map and dip length measured on cross section of a thrust
L arc length of thrust dislocation within a particular stratigraphic interval
M metamorphic quantity
n_j component of outwards surface normal

r grain axial ratio
S surface area
t time
T absolute temperature
u, u_j, $\bar{u}$, u^* displacement, displacement component, mean displacement, transitional displacement
V, V_j volume and volume element
V_c, V_p volume of ductile bead and volume swept out by bead during growth of thrust
W deformation work in general, when primed represents work calculated on a cross section of unit thickness
W_g, W_s, W_i work of gravitational and surface forces on the thrust system, and deformation work within interior of sheet
W_c, W_p, W_b work to create, propagate and slide along on thrust fault surface V, V_j
x_i rectangular coordinates
α dip of topographic surface of thrust sheet
γ general measure of finite shear strain intensity, a bar indicates average value, a dot indicates shear strain rate
$\bar{\gamma}_c$, γ_f average shear strain and shear strain at fracture within volume of ductile rock V_c
γ_t shear strain in wall rock adjacent to thrust
δ thickness of grain boundary or solution film
η coefficient of shear viscosity
λ ratio of pore pressure to normal stress on the surface
μ coefficient of sliding friction
ρ density
σ_{ij} elements of stress tensor
τ general shear stress intensity, a bar indicates average value
τ_b, $\bar{\tau}_i$ basal shear stress and mean shear stress within interior
$\bar{\tau}_s$ average shear stress on boundary due to surface forces
τ_y yield or flow stress for deforming rock
τ_n, σ_n shear and normal stress on surface whose normal is n
τ', τ^0 constants with dimensions of shear stress
ϕ slope of Mohr–Coloumb yield envelope on Mohr Diagram
Ω atomic volume

Introduction

Three principal aims of this paper are to calculate the mechanical energy consumed in the emplacement of a thrust sheet, to see where in the thrust sheet this energy is dissipated, and to find out how, or by what process, the energy dissipation occurs. In addition I wish to present some ideas on how the thrust fracture surface arises.

As in so many problems in structural geology the key lies in proper deciphering of the geometry and sequences of structural events within a thrust complex. Many of these 'rules' have been developed in the Canadian Rockies in a literature scattered through several journals and guidebooks, in part summarized by Dahlstrom (1970).

In addition to the powerful methods for determining the structural geometry and sequence of events, some progress into understanding the emplacement of thrusts can be made purely

from considerations of static equilibrium. For example, an entire thrust sheet is so long in cross section (*ca.* 100 km) and contains so large a volume of rock that, compared to the effect of gravitational forces, any conceivable compressive surface force exerted from the hinterland is of negligible importance in effecting forward motion. Consequently, it is possible to write a simple equation for the basal shear stress operating along a thrust fault (Elliott 1976*a*). But only limited progress can be made from statics alone and further progress is hindered by our lack of knowledge of the constitutive equations appropriate for deforming rocks.

It is frequently suggested that the detailed stress distribution and motion along the thrust may be controlled by a dislocation type mechanism. The importance of such dislocation mechanisms along thrust fault surfaces was first suggested in a general way by Oldham (1921) and Hubbert & Rubey (1959). Barnes (1966) and Price (1973) have emphasized the importance of this point of view. Creeping-type slip for various kinds of faults has been modelled in a number of ways with groups of smeared-out dislocations (e.g. Nason & Weertman 1973).

But all these dislocation models require an explicit statement of the appropriate constitutive equations for the sliding surfaces, the tectonic breccia, or the wall rock, as the case may be. There seems to be little advantage in using bold assumptions about ancient sliding surfaces until the constitutive equations can be brought at least into sharper focus, and it is pointed out in this paper that progress is possible in this direction purely from field observations.

Some of these difficulties may be overcome by looking at the energy balance of a thrust sheet and seeing how it is partitioned among the various processes. If surface forces are insignificant compared to gravitational forces, then the work expended in emplacing a thrust sheet must be provided by a decrease in the potential energy of the thrust mass. By comparison of the initial and final potential energy of the thrust we may measure the amount of energy expended in mechanical deformation. Such an approach was pioneered by Goguel in 1948 and applied by him to a number of thrust complexes in the French Alps, but does not seem to have been used since then. Unfortunately, few techniques for working out the structural geometry were available at the time and several complications in Alpine geology made determination of the initial and final states of these thrust sheets rather imprecise.

The McConnell thrust system

The first objective is to define the thermodynamic system as it existed between the original state just before motion along the particular thrust until the final state following a thrust's activity. This thrust system is specified by the four boundaries listed below (figure 1).

1. The top boundary lies along the surface where all elements of the stress tensor σ_{ij} are zero.

2. Thrust sheets lose mass by erosion, but it has been shown that during motion of a thrust most of this erosion occurs from the vicinity of the toe (Price & Mountjoy 1970).

Thrust sheets also gain mass by successive imbrication into the footwall rocks below and in front of the current outcrop of the thrust. In order to avoid problems with this large mass transfer occurring in the vicinity of the toe, we will define the front boundary as the material surface in the original state which will eventually become the topographic front surface in the final state. This type of boundary is quite general, yet has the advantage of defining a closed system – or one of constant mass.

3. The lower boundary lies within the footwall below the thrust surface.

Below this boundary are undeformed rocks structurally attached to the foreland, and above is a thin rind of footwall rocks deformed by passage of the thrust sheet. Along this lower boundary, all strain and displacement components are zero ($u_j = 0$).

4. In the original state the trailing edge boundary is a vertical material line chosen to enclose a volume of rock of interest. Since the thrust system is assumed to be undergoing plane incompressible flow, a vertical line in the final state chosen to enclose the same volume as the initial state will give the average position of the trailing edge boundary but not its curved shape.

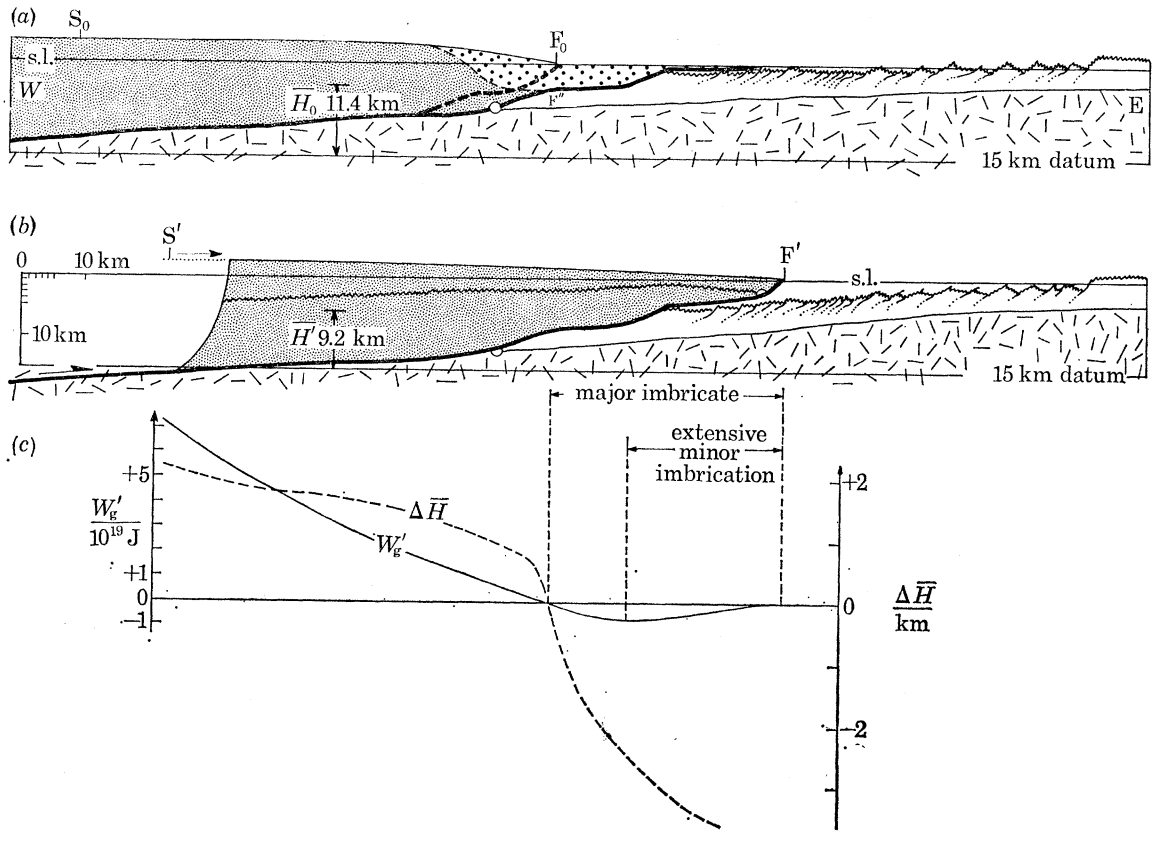

FIGURE 1. (*a*) Bow Valley cross section from the planes into the Western Main Ranges in the Early Maestrichian 'original state' before motion along the McConnell thrust. F_0 and S_0 are the mountain front and 3500 m topographic summit. F″ is the original position of the hanging wall beds which will be at the mountain front F′ in the final state. Height H_0 of the centre of gravity is 11.4 km above the −15 km horizontal datum. The present erosion surface is shown as a serrated line. Location of section shown on figure 4.

(*b*) The final state in the latest Maestrichian after motion on the McConnell. F′ and S′ are the mountain front and the 2500 m topographic summit. The centre of gravity H' is 9.2 km above the horizontal datum.

(*c*) Graph of W'_g and ΔH with horizontal position in the final state. The major imbricate slice in figure 1*b* coincides almost exactly with $W'_g \simeq 0$. The front toe has its centre of gravity raised. The toe portion is dominated by extensive minor imbrication, but this is not shown.

However, a substantial component of simple shear parallel to bedding is a direct geometric consequence of a thrust surface cutting up section in the direction of motion (figure 2). This effect imparts a strong curvature to the trailing-edge boundary and will be discussed later in the paper.

With our thrust system defined, we can now look at the forces which produce changes in shape and position of this system. The external forces are of two possible sorts.

1. Gravitational forces acting on the mass of the thrust system. Positive gravitational work W'_g is accomplished on the system whenever the centre of gravity is decreased from the initial to the final state.

2. Surface forces may accomplish work W'_s on the boundaries of the thrust system.

The total work by all the external forces is the sum of two terms,

$$W' = W'_g + W'_s \tag{1}$$

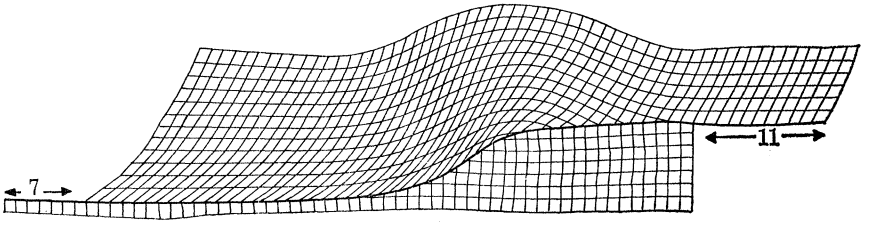

FIGURE 2. Originally rectangular grid stamped onto a stack of paper and cut by a thrust fault. Trailing edge moves forwards 7 units along thrust and necessarily assumes a concave shape. Leading edge along thrust moves forward 11 units. Note the widespread distribution of simple shear strain as a result of movement over this footwall step. (Drawn from photograph.)

Both of these external forces act very slowly, therefore inertial terms are negligible and mechanical equilibrium is attained between the system and the surroundings. Consequently, the total work by all the external forces is exactly balanced by the work of internal forces which resist this motion and deformation of the thrust sheet. This internal work is used up in shearing motions completely and irreversibly and is dissipated as heat, i.e. shear-strain heating.

We will now calculate the gravitational work W'_g for the McConnell thrust in the Canadian Rockies, then we will consider the effects of work by surface forces.

The section westwards from the Bow River passes through the central part of the McConnell thrust (figure 4). Along this line, original and final state cross sections were constructed (figure 1) based upon the restored section by Bally *et al.* (1966, plate 12), in turn supported by published seismic sections.

The thrusts making up the Foothills, Front and Main ranges were developed during deposition over a 50 Ma time span from Campanian to Oligocene of the synorogenic Belly River-Paskapoo assemblage, the second major molasse sequence deposited in the Canadian Rockies (Eisbacher *et al.* 1974). Foothill thrusts cut the Paskapoo Formation but are overlain by the Porcupine Hills (Carrigy 1971); this dates the Foothill thrusting between 65–60 Ma ago. The Foothill thrusts deform and therefore post-date the McConnell and must have ceased activity about 65 Ma ago. The McConnell thrust at Black Rock has a good portion of the lower Brazeau Formation (Lower Maestrichian) as footwall and the thrusting here must be after about 72 Ma ago. Consequently the toe of the McConnell thrust was active over at most an 8 Ma time span. Its displacement is about 40 km, giving a minimum mean velocity of 5 mm/a or 1.6×10^{-10} m/s.

The effects of Foothill thrusting may be removed by constructing a restored section (Bally *et al.* 1966, plate 12) to establish the undeformed trajectory of the McConnell thrust. The eroded portion was reconstructed by allowing the toe of the McConnell to climb in the lower Brazeau Formation with the characteristic stairstep fashion shown by nearby Foothill thrusts.

As a thrust sheet advances so much mass is transferred laterally along the crust that a large

isostatic depression spreads far out in front of the thrust outcrop; such isostatic depressions are a dominant feature in controlling molasse basins (Bally *et al.* 1966; Price & Mountjoy 1970; Price 1974). The depoaxis of successive molasse foredeeps migrate cratonwards, driven by the isostatic response to a moving thrust mass.

Sealevel at a given time can be estimated from the shallow water, alternatively fresh and marine, formations. Restored sections for various times can then be drawn using the different estimated sealevels as horizontal datum. This has been done for the Early Maestrichian (*ca.* 74 Ma), before motion on the McConnell (figure 1*a*), and for the latest Maestrichian (*ca.* 62 Ma), not long after motion ceased (figure 1*b*). The sealevel lines must be projected for considerable distances without any preserved evidence – a procedure which is probably the chief source of error. Other sources of error are numbered below. The current erosion level is close to the Early Maestrichian time line so that this section is much more soundly based than the latest Maestrichian one. The isostatic depression is observed to increase rapidly westwards; but this cannot be maintained forever and the angle of dip of the décollement to the west is taken to gradually approach its current dip.

The thrust induced isostatic depression becomes strikingly clear on these restored sections (figure 1). By creating a depression ahead, thrusts make it much easier to move themselves forwards; indeed it is doubtful if the McConnell thrust could have moved at all without this isostatic adjustment. Since the horizontal datum can be fixed for both original and final states, this isostatic response is implicitly accounted for in the gravitational work calculations.

In the original state, the mountain front was assumed to start at the thrust which outcrops immediately west of the McConnell. The mountains were assumed to have a relief of 3500 m, no higher than the relative relief today between the Andes and its eastern craton. The surface slope was drawn at an average of 2.5°, steeper at first and then tapering off. In the final state, the mountain starts at the surface outcrop of the McConnell and rises to 2500 m with an average surface slope of 1.5°. Such reconstructed surfaces are clearly a source of error (2), although judging by contemporary active mountain belts there is not too much room for a significantly different surface topography.

The geometry of the thrust sheet is subject to increasing error (3) west of the Continental Divide, where listric normal faults become important and probably post-date development of the McConnell. For this reason, the system is arbitrarily terminated about 6 km east of the Trench. The concave shape of the trailing edge boundary in the final state is an estimate also subject to error (4). The trailing edge boundary to the original state is drawn so as to enclose a volume equal to that of the final state of 1.1×10^3 km^3. We assume that both original and final state cross sections are 1 km thick perpendicular to the plane of section.

Prior to being displaced 40 km along the McConnell thrust, point F′ in the final state was once at position F″ in the original state. The position in the original state of the material points in the deformed final state which make up the rest of the topographic surfaces S′ F′ may be estimated and the uneroded mass below and to the west of S_0 F″ is the original position of that volume of rock which became the McConnell sheet. This front boundary again is subject to error (5).

The thin layer of the footwall which is part of the thrust system has a very small volume in comparison to the rest of the system, nor does this volume undergo much change of its centre of gravity. Its contribution to the gravitational work may be safely neglected.

The gravitational work of the rest of the thrust system may now be calculated by the classical

PHILOSOPHICAL TRANSACTIONS OF THE ROYAL SOCIETY A MATHEMATICAL, PHYSICAL & ENGINEERING SCIENCES

methods. Draw a horizontal datum line 15 km below the reconstructed sealevel on each section (figure 1). The cross sections can now be subdivided into convenient 10 km long elements and the volume V_j, centre of gravity H_j of each element measured.

Then starting from the toe and moving towards the hinterland the cumulative volume V,

$$V = \sum_0^j V_j$$

has a centre of gravity H,

$$H = \sum_0^j V_j H_j \Big/ V. \tag{2}$$

The difference in the centre of gravity between the original H_0 and final H' states is for a particular volume of rock

$$\Delta H = H_0 - H'.$$

This ΔH is plotted with respect to position in the final state (figure 1*c*).

The work accomplished by gravity W'_g for an equivalent volume V in the original and final states is

$$W'_g = \rho g V \Delta H. \tag{3}$$

This gravitational work is also plotted with respect to position in the final state (figure 1*c*). Note that from equation (3) gravitational work per unit volume (W'_g/V) varies directly with change in centre of gravity, so that ΔH is a measure of energy density.

How accurate are these results, particularly in view of the five numbered geological sources of error indicated in the text above? The largest error undoubtedly arises during restoration to sealevel. Although exact limits to this and the other errors cannot be given, trials with various 'worse possible' cross sections did not change the order of magnitude of the gravitational work. Note also that for a western boundary anywhere within the last 60 km of the thrust sheet, the gravitational work is in the order of 10^{19} J. It appears as if errors might not give rise to wildly fluctuating results, and the value of 10^{19} J would be attained even after moderate alterations to the cross sections.

Errors of measurement from the cross sections are comparatively small, and it is in this sense that the gravitational work is reported to two significant figures.

The work of surface forces can only be applied at the boundaries of the thrust system. At such a boundary

$$W_s = \int_0^S u_j \sigma_{ij} n_j \, \mathrm{d}S \tag{4}$$

where the displacement component is u_i, stress component σ_{ij}, the outward normal n_j, and the surface area of the boundary is S.

Now consider the 4 bounding surfaces of the thrust system. The top surface is stress free $\sigma_{ij} = 0$, the lower boundary is deformation free $u_i = 0$, and the front boundary is close to the surface so that the stress σ_{ij} and displacement u_i are small. The only part of the boundary of the thrust system on which surface forces may accomplish work is the trailing edge boundary. In other words this is the 'principal' boundary condition because the state of the surface forces on this boundary specifies the prime agency generating the motion of the thrust (see, for example, Batchelor 1965, p. 217). We represent these surface forces by a stress whose magnitude is zero at the surface and might reach a maximum value limited by the shear strength of the rock of 2.5×10^7 Pa at the thrust fault. This stress is largely a deviatoric shear stress. The

maximum long term average regional shear stress $\bar{\tau}$ for an entire sheet is in the order of 10^7 Pa (Elliott 1976*a*). Equation (4), when applied to the trailing edge boundary, may be expressed as

$$W'_s = u\bar{\tau}h\,\mathrm{d}x_3. \tag{5}$$

Here the area of the trailing edge boundary is the height h times the arbitrary thickness $\mathrm{d}x_3$ normal to the plane of section and u is displacement of the top with respect to the bottom of the trailing edge boundary.

Recall that the total work expended is the sum of gravitational work and the work accomplished by the surface forces. This work W' must be positive:

$$W' = W'_g + W'_s. \tag{1}$$

There are three special cases of this exact equation, and we will now see that each of these cases applies to natural subdivisions of the thrust system found on the cross sections and graphs (figure 1).

(1) One of the main theories for thrusting is that it occurs as a result of *longitudinal compressive surface forces*. One form of this theory is expressed as

$$W' = W'_s - W'_g > 0. \tag{6}$$

In this case the centre of gravity is raised so gravitational work is negative. Much of the work exerted by surface forces is consumed in overcoming this gravitational resistance. This special case clearly applies to the front 150 km^3 toe region of the McConnell thrust, where the centre of gravity is raised as a result of deformation, and the gravitational work is negative with a value of -7.5×10^{18} J (figure 1*c*). The magnitude of the gravitational energy density reaches higher values here than anywhere else in the thrust system.

The toe of the McConnell thrust almost certainly resembled the swarm of minor imbricates marking this stratigraphic level in the foothills. This extensive minor thrusting proves that the thrust sheet is losing coherency or unity, suggesting that the stress $\bar{\tau}_s$ is greater than 10^7 Pa in this region; in fact if $\bar{\tau}_s \approx 2.5\times10^7$ Pa then the work of surface forces acting on this front toe region would be 8×10^{18} J, which is enough to overcome gravitational resistance.

(2) Another form of the *longitudinal compressive surface force theory* is

$$\left.\begin{aligned} W' &\approx W'_s \\ W'_g/W'_s &\ll 1. \end{aligned}\right\} \tag{7}$$

For the 230 km^3 front portion of the thrust sheet the gravitational work W'_g is approximately zero. The decrease in local centres of gravity $\bar{H}_j$ of volume elements V_j (see equation (2)) at the back of this region are enough to raise the centre of gravity of the toe, and no net gravitational work is produced or consumed.

The major imbricate of 230 km^3 is about 11 km thick at its trailing edge. The maximum possible work by the surface forces here, from equation (4), is about 5.6×10^{18} J.

(3) The final special case of equation (1) is the *gravity spreading theory* which may be stated as 'the driving force for thrust emplacement is entirely a consequence of the sheet's weight'. For this case

$$\left.\begin{aligned} W' &\approx W'_g \\ W'_s/W'_g &\ll 1. \end{aligned}\right\} \tag{8}$$

The main body of the sheet, 1.1×10^4 km^3 is about 15 km thick at its trailing edge, so that the maximum possible work of the surface forces on this system is 6×10^{18} J.

From the volume of about 300 km³ upwards, gravitational work is expended by the motion of the sheet and is of the order of 10^{19} J for the entire western 60 km of this sheet. For the sheet as a whole (1.1×10^3 km³) the centre of gravity fell through 2.2 km and $+7.3 \times 10^{19}$ J of gravitational work was expended, an order of magnitude greater than any possible work of surface forces. In summary, this special case of gravity spreading will apply for either the whole of the McConnell thrust system or the frontal portion, so long as it is greater than about 300 km³. Small portions near the front involve substantial longitudinal compressive surface forces. What seems to be happening is that the surface forces acting on the toe region and on the major imbricate are themselves provided by the gravitational forces acting on the main mass. The prime agency is gravity, but on a smaller scale the longitudinal compressive surface force theory is also clearly applicable. It all depends on the volume of material considered within the thrust system.

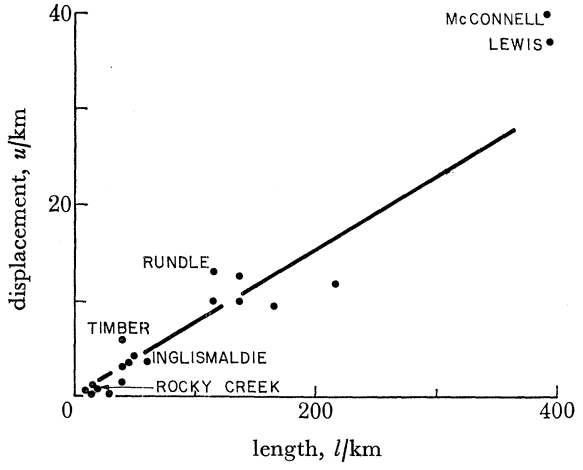

FIGURE 3. Maximum displacement u in central part of a thrust versus map length l for 20 thrusts from the foothills and front ranges. A linear relation is suggested. The named thrusts are referred to in the text and subsequent figures. Further data, statistical analysis, and a detailed bibliography are presented elsewhere (Elliott 1976*b*).

THE INITIATION AND GROWTH OF A THRUST SURFACE

I have plotted in figure 3 the maximum stratigraphic separation observed along thrusts in cross section versus their map length for 20 thrusts in the foothills and front ranges of the Canadian Rockies. The main criteria in choice of a particular thrust to plot were (*a*) the existence of fairly recent cross sections and maps and (*b*) thrusts without complex splays. Faults whose map pattern showed extensive branches proved awkward to handle and they seemed to plot much more irregularly. Nevertheless, I believe the particular thrusts chosen are reasonably repesentative. There are several implications from this graph.

(1) It has been suggested for some time that 'long thrusts are strong thrusts'. We see here that in fact not only do the longest thrusts have the largest displacements, but there is a roughly linear relation between strike length l on the map and displacement u,

$$u \simeq Kl \tag{9}$$

where $K \simeq 7\ \%$.

(2) Presumably thrusts in all different stages of growth are present on this graph. As Douglas (1958, p. 130) pointed out, a thrust starts as an initial break at a given point and

spreads out sideways in both directions. Consequently this relation (9) must apply to the development in time of a given thrust.

$$du/dt = K\,dl/dt.$$

(3) The initial break is roughly in the centre of the map length and the maximum displacement must be at this point. This is clearly demonstrated by the McConnell thrust (figure 4) where the displacement is 0 at its northern termination, reaches a maximum, then loses displacement towards its southern termination.

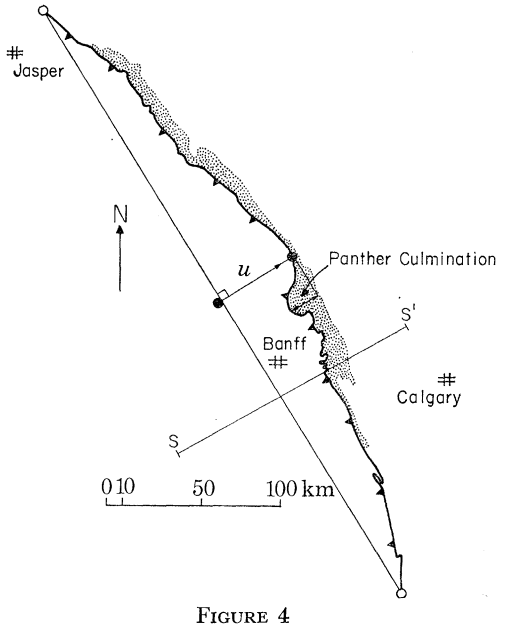

FIGURE 4

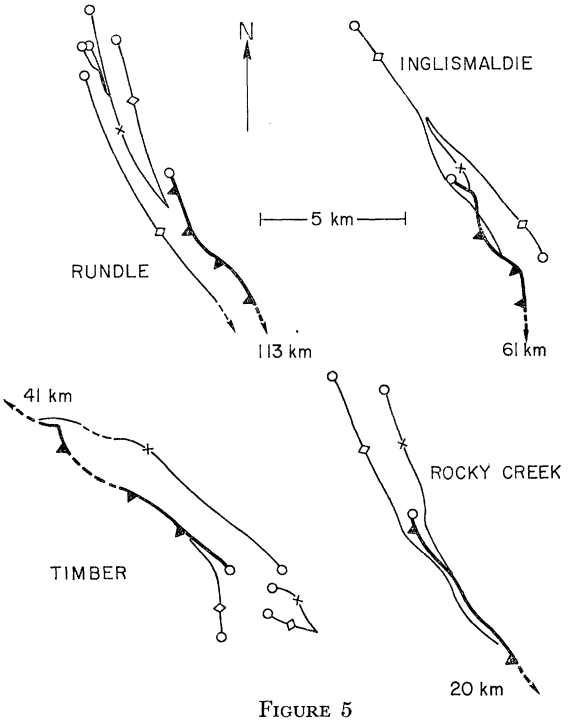

FIGURE 5

FIGURE 4. Map of the McConnell thrust, which has a strike length of 410 km. The re-entrant at the Panther culmination gives an absolute minimum displacement of 20 km. The balanced cross section of figure 1 is through S–S′ and along this line displacement $\simeq$ 40 km. The chord joining the 2 ends of the thrust has a normal bisectrix, and along this bisectrix, by the 'bow-and-arrow' rule, lies the maximum displacement $u \simeq 45$ km of the thrust. In the central portion of the McConnell thrust the hanging-wall is Middle Cambrian shelf carbonate facies and the footwall is Cretaceous molasse (stippled). Towards the ends one goes up section in the hanging-wall and down section in the footwall, and the terminations of the thrust are in Devonian–Permian shelf carbonates. Fold complexes at the ends of the thrust are not shown.

FIGURE 5. Maps of fold crest and trough surface traces near the ends of 4 thrusts in the Foothills and Front Ranges. All the fold complexes die out about 8 km ($= a$) from the end of the thrusts. The ends of the thrusts are about 0.5 km ($= \frac{1}{2}b$) from adjacent crest and trough surface traces. Note that a and b are about the same size regardless of size of thrust.

(4) The direction of this maximum displacement vector u on a map is the normal bisector of the straight line joining the two ends of the particular thrust. I call this the 'bow and arrow' rule.

(5) Stratigraphic evidence (such as given earlier for the McConnell) indicates that thrusts move between 10^{-10} and 10^{-9} m/s, from equation (9) the rate of lateral propagation of the thrust $dl/dt \approx 10^{-11}$ to 10^{-12} m/s. In other words, *thrust fracture surfaces propagate very slowly*.

This process of slow, lateral growth of the thrust fault can be clarified by studying the way thrusts die out, summarized in the following points.

(6) It has been known at least since Heim (1921) that thrusts die out along strike into folds.

(7) These folds are strongly non-cylindrical with both converging and diverging hinges. Fold pairs are linked in the sense that as antiform and synform converge the folds become tighter and tighter towards a singularity. Thrusts usually pass through such singularities (Ollerenshaw 1968).

(8) These fold complexes have characteristic dimensions, regardless of the length of the thrust. For example figure 5 shows fold complexes dying out about 5–10 km from the end of the thrusts (dimension b) and a typical distance from the fold hinges to the end of the thrust is about 0.5 km (dimension $\frac{1}{2}a$).

(9) Where thrusts die out in the overturned short limbs of asymmetric folds ('forelimb thrusts') finite simple shear strains are fairly high, $\gamma_f \approx 1$.

When thrusts die out in the right-way-up long limbs ('backlimb thrusts') the finite simple shear near the fracture is considerably less, $\gamma_f \simeq 0.1$. This strain γ_f is estimated assuming that the asymmetric folds are of flexural-slip type, and regardless of the length of the thrust and its maximum displacement the shear fracture strain γ_f appears to be roughly constant.

(10) The magnitudes of a, b and γ_f cited above are for the very low grade rocks of the Foothills and Front Ranges. As the metamorphic grade increases, the values of a, b and γ_f probably change, all increasing as the ductility of the rocks increases.

From these last 6 observations (6 to 11), we may conclude that a non-cylindrical fold complex travels just ahead of a sideways propagating thrust. The rocks are folded, the folds grow and tighten, and then the thrust fracture extends laterally into this strained mass. The folds indicate that ductile deformation of substantial magnitude affects the rock before the crack slowly propagates into it. Presumably, as the strain progresses, *damage* accumulates. Preliminary field work suggests that in some instances this damage is caused by minor tension fractures which become steadily larger, more numerous, and record higher strains towards the thrust. Eventually these flaws reach a stage where they suddenly run together forming the large scale thrust fracture. The propagation of thrust faults appears to be a case of *ductile fracturing*, and the most widely used ductile fracture criteria is that of a limiting finite strain above which a fracture appears as the coalescence of flaws (*see* MacClintock & Argon 1966, for a good review).

Odé (1960, p. 300) defined purely ductile faults to be those for which there is no stored elastic strain energy; an assumption precisely opposite to what one would make for a Griffith-type purely brittle fault. Odé suggested thrusts as examples of purely ductile faults; his plastic analysis is rather different from the approach presented below.

A key relation is that the distortional work W due to a particular rock deformation mechanism affecting a volume V of rock can be expressed in terms of the octahedral shear stress τ and strain γ as

$$W = \frac{3}{2}\int_0^V \int_0^\gamma \tau \, \mathrm{d}\gamma \, \mathrm{d}V. \tag{10}$$

This equation expresses the fact that the work is dependent upon the path of finite strain γ.

Throughout the rest of this paper we shall assume simple shear paths for ease of discussion, but this in no way restricts the physical reasoning. Further, deformation paths are a measurable quantity in naturally deformed rocks. For example, the fold complex at the thrust tip may be observed to be of flexural slip type so that the deformation path is one of simple shear along bedding. Alternatively, in penetratively deformed rocks the deformation path can be measured from fibres (Elliott 1972; Durney & Ramsay 1974).

PHILOSOPHICAL TRANSACTIONS OF THE ROYAL SOCIETY A MATHEMATICAL, PHYSICAL & ENGINEERING SCIENCES

The local shear stress must have been higher in the ductilely deformed fold complex than its regional value in the much less deformed rocks outside the immediate vicinity of the thrust termination. This local stress would be reached by the stress concentrating abilities of the fracture. If we assume that a characteristic flow stress τ_y had to be achieved to produce the ductile flow within these fold complexes, some interesting conclusions can be drawn. Note that use of such a flow shear stress may be justified in three different ways:

(1) In an exact sense, as a shear stress averaged over both time and through the volume of ductilely deformed material,

$$\tau_y = \frac{1}{tV}\int_0^t \int_0^V \tau \, dt \, dV.$$

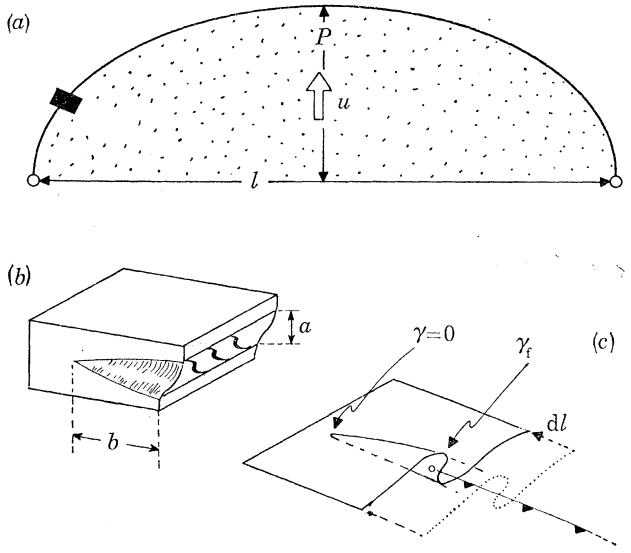

FIGURE 6. (*a*) Plan view of thrust. The thrust surface is stippled. Displacement reaches a maximum u in the central region. The perimeter of the thrust surface is the thrust dislocation, and outside of this perimeter the formation is unfaulted. The thrust dislocation is assumed to be a half ellipse enclosing an area $(\frac{1}{4}\pi)\,pl$ where p and l are the dip and strike lengths of the thrust surface within the formation. (*a*) and (*b*) examine various detailed aspects of the black rectangle.

(*b*) Schematic view of portion of formation just beyond thrust. Ductile deformation zone dies out in distance b and is of thickness a. Strain damage suggested by sigmoidal tension cracks, shown black within deformation zone. This type of ductile bead lies all along thrust dislocation.

(*c*) Folds in formation at end of thrust shown by thin marker layer. Thrust has lengthened by moving distance dl into previously deformed rock. Finite strain at fracture $\gamma_f \approx 0.6$ here where the interlimb angle $\approx 60°$. Fold dies out at point of zero, strain ($\gamma = 0$) over length a.

(2) In an exact sense again, as the shear yield stress in a perfectly plastic rock.

(3) In an approximate sense, as the yield stress of the perfectly plastic approximation to a power law material, $\dot{\gamma} \propto \tau^n$. This approximation is good whenever $n > 3$.

For a simple shear deformation path, with τ_y and γ measured in the simple shear direction,

$$W = \tfrac{1}{2}\tau_y \gamma V. \tag{11}$$

The tip which surrounds an active thrust separates faulted from unfaulted rock and is a type of fracture dislocation (figure 6). This fracture or 'thrust dislocation' has edge character in the central region and screw character at both sides. The central tip of the thrust dislocation

eventually climbs out of the formation and may reach the ground surface, splitting the thrust dislocation into two parts each of essentially screw character. The screw type component affects a particular formation as if it were being torn like a sheet of paper.

We shall now see that the region of deformed and folded rocks at the ends of thrusts provides insight into how a thrust within a particular formation is created, propagated and slowly grows.

(*a*) *Creating the thrust fracture*

We have seen field evidence which indicates a lip or 'bead' of ductile rock all along the thrust dislocation. This bead has thickness a, breadth b, and cross sectional area $\frac{1}{4}\pi ab$ (figure 6). With arc length L of thrust dislocation within the formation, then the volume V_c of the ductile bead is

$$V_c = \tfrac{1}{4}\pi abL.$$

The work W_c necessary to produce a shear strain $\bar{\gamma}_c$ averaged over this ductile volume V_c, assuming a simple shear deformation path

$$W_c = \tfrac{1}{4}\pi \tau_y \bar{\gamma}_c abL.$$

The work W_c' to create the part of the ductile bead within the cross section slice which is dx_3 thick is

$$W_c' = \tfrac{1}{4}\pi \tau_y \bar{\gamma} ab\, dx_3.$$

For the entire McConnell thrust system, $\tau_y \simeq 2 \times 10^7$ Pa, $\bar{\gamma} \simeq 0.25$, $a \simeq 1$ km, $b \simeq 8$ km (from figure 5), $dx_3 = 1$ km, so $W_c' \simeq 1.6 \times 10^{16}$ J.

(*b*) *Propagating the thrust fracture*

Over its active life the dislocation bounding the edge of the thrust surface sweeps out an area of $\frac{1}{4}\pi\, pl$ (figure 6). But in order to move this thrust dislocation forwards or sideways, the ductile bead of thickness a must move ahead of the propagating fracture and sweeps out a volume V_p

$$V_p = \tfrac{1}{4}\pi apl.$$

This entire volume of rock reached the finite strain necessary to induce ductile fracture γ_f; assuming a simple shear deformation path the work W_p necessary to push this ductile zone ahead is

$$W_p = \tfrac{1}{8}\pi \tau_y \gamma_f apl. \tag{13}$$

For a cross-section slice of thickness dx_3 the work W_p' is

$$W_p' = \tfrac{1}{2}\tau_y \gamma_f ap\, dx_3. \tag{14}$$

For the McConnell thrust system, if the finite strain before fracture $\gamma_f \simeq 0.5$ (figure 5), $p \simeq 90$ km, and for a slice of 1 km thick, $W_p' \simeq 8.8 \times 10^{17}$ J.

Increase in ductility of the rock would be reflected in higher values of a, b, $\bar{\gamma}$, γ_f, V_c and V_p, and in a lower value of the yield stress τ_y. This increase in ductility affects the work both to create and to propagate a thrust.

We saw that the sides of a thrust dislocation are essentially of screw character, and in fact resemble the 'tearing' or 'mode III' type problem in fracture mechanics. Fortunately this is one of the few problems in ductile fracturing for which analytical solutions exist. This problem is briefly discussed, for example, in MacClintock & Argon (1966, p. 409) where assuming a perfectly plastic

ductile bead which just touches the crack tip and is of circular diameter d, they derive that $d \propto \tau_y^{-2}$ and $\gamma_f \propto \tau_y^{-1}$. Thus α and $b \propto \tau_y^{-2}$ and $W_c \propto \tau_y^{-4}$, $W_p \propto \tau_y^{-2}$, and a small increase in ductility causes a large increase in the work necessary to create and propagate thrusts. In zones of high grade metamorphism one should expect to see less thrusting. Field work seems to bear this out; in fact, structural mapping in higher grade rocks often reveals that any thrusting which occurred did so at an early stage under very low grade metamorphic conditions.

(*c*) *Sliding on the thrust surface*

The work W_b involved in sliding along the base of area $\frac{1}{4}\pi lp$ is

$$\tfrac{1}{4}\pi\tau_b p l\bar{u}.$$

Note that we have defined this basal sliding work in such a way that it occurs only along the thrust, a two dimensional surface of zero thickness.

Evaluation of the mean displacement $\bar{u}$ is important. Consider first the average along the dip length p.

Study of figure 2 reveals that the trailing edge has less thrust displacement than the leading edge. The central portion of the model thrust cuts steeply up section in the hanging wall and in this region simple shear from within the body of the sheet is transferred to displacement along the base.

We seem to have a method whereby simple shear within the body of the sheet can be converted into displacements along the base, so that the thrust surface gathers slip as it cuts up section. A large proportion of the observed 40 km displacement observed at the leading edge of the McConnell could die out down dip.

Another feature which we must take into account is that the displacement along the leading edge of a thrust reaches a maximum value u in the central part and dies out at each end over a strike length l (figure 4). Assuming that the variation in displacement with strike length traces a semiellipse, the value of the displacement averaged over the strike length is $\frac{1}{4}\pi u$.

Averaging over the dip and strike lengths,

$$\bar{u} = C\tfrac{1}{4}\pi u.$$

Here $C < 1$, and accounts for the thrust gaining displacement as it cuts up section. Therefore

$$W_b = C(\tfrac{1}{4}\pi)^2 \tau_b p l u. \tag{15}$$

On a cross section the thrust surface has an area $p\,\mathrm{d}x_3$ and the work of basal sliding W_b' is

$$W_b' = C\tau_b u p\,\mathrm{d}x_3. \tag{16}$$

It was demonstrated in a previous article that the shear stress acting on the base of a thrust sheet τ_b is (Elliott 1976*a*).

$$\tau_b \simeq \rho g h \alpha \tag{17}$$

where α is the surface slope. This basal shear stress τ_b represents an average value over a distance along the base several times the local thickness h of the sheet. A typical value for the basal shear stress along the sole thrust in the southern and central Canadian Rockies was estimated at about 5×10^6 Pa, probably higher at the beginning of thrusting and dropping towards the end.

For the McConnell thrust (figure 1) C is unknown; a value of 0.5 might be reasonable and in this case $W_b' \approx 9 \times 10^{18}$ J.

(*d*) *Growth of a thrust*

When a thrust is first starting to grow within a formation the relative importance of the work terms W_b, W_p, W_c may be quite different from the later, large displacement stage.

The conditions under which $W_b = W_p$ is found by equating equations (15) and (13). The transitional displacement u^* is

$$u^* = 2/\pi C(\tau_y/\tau_b)\ \gamma_t a. \tag{18}$$

By equating equations (11) to (13), and using equation (9), the conditions under which $W_c = W_p$ is

$$u^* = K(\bar{\gamma}_c/\gamma_t)\ (L/p)\ b. \tag{19}$$

Substituting in appropriate values for the Foothills and Front ranges we find that the transitional displacements u^* are about 1–2 km. For small thrusts with displacements below these values the work required to create the fracture surface is a dominant term, $W_c > W_p > W_b$. For displacements above these transitional displacements, $W_b > W_c > W_p$, and in the previous section we found that for the entire McConnell thrust system with $u \approx 40$ km that $W'_b > W'_p > W'_c$.

(*e*) *Deformation within the main body of the sheet*

A simple way of visualizing the resistance set up within the mass of the thrust is to imagine a situation where the base of the sheet was perfectly lubricated so that there could be no basal terms W_c, W_p, W_b. Nevertheless, everytime the thrust went over a substantial bump or obstacle in the base, the entire sheet would have to be deformed into conformity with the bump so that no voids would open up. At low metamorphic grades such deformation would be essentially flexural slip folding (parallel to kink folds) with sliding on a large number of discrete surfaces set up throughout this portion of the thrust sheet.

Another and possibly greater source of internal deformation is the simple shear within the thrust sheet which must be transferred to the base as the thrust cuts up section (figure 2).

There are, then, two types of deformation within the sheet which must proceed in order for basal sliding to occur without continuity being destroyed or holes opening up. During basal sliding internal deformation is therefore a necessary process, or in other words, basal sliding and internal deformation are *dependent processes* and the overall rate determining step is the slowest of the two. It seems that the internal slip which must be activated over the huge area of internal surfaces such as bedding within a thrust sheet makes this internal deformation the rate limiting step.

On balancing the external work provided to the internal work expended within the system, assuming gravity spreading (equation 8),

$$W' \simeq W'_g = W'_i + W'_b + W'_c + W'_p.$$

For the McConnell thrust system the last two terms W'_c, W'_p are two or three orders of magnitude less than the second term W'_b, and by subtraction $W'_i \simeq 6.4 \times 10^{19}$ J. But is it generally true that $W'_i > W'_b$? The evidence is at least suggestive, but information on the strain distribution within thrust sheets is essential. Much of the resistance to forwards motion of the sheet may lie here.

Now we wish to determine by what physical processes this deformation occurs. It is useful to classify the mechanisms of deformation operating within thrust systems depending upon whether slip on discrete surfaces or continuous deformation of some finite volume is

involved. In the next sections we will look at the mechanical processes involved in these kind of deformation, using the 'flow chart' (figure 3) as a guide.

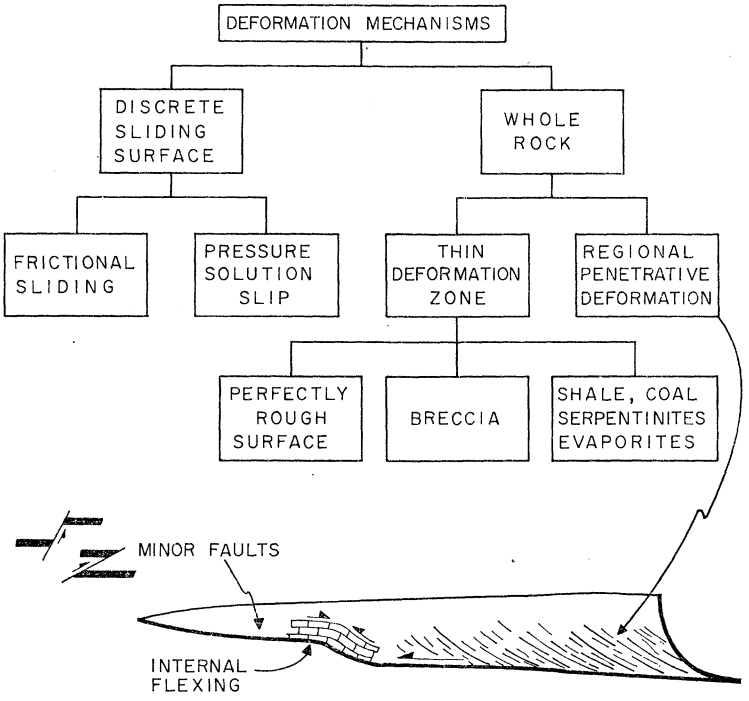

FIGURE 7. One manner of classifying the various kinds of deformation mechanisms occurring in a thrust system. Discrete sliding surfaces include bedding planes and minor faults. Slip is activated as the thrust climbs section.

DEFORMATION BY SLIP ON DISCRETE SURFACES

These discrete sliding surfaces appear to the eye to have no thickness, and the rock in between two such sliding surfaces undergoes little deformation.

Essentially undeformed fossils and oolites occur within a few metres of major thrusts such as the Pulaski and Saltsville in the central Appalachians. These observations were made within individual bedding units, and simply proves that internal deformation within the thrust sheet must have occurred by slip along discrete surfaces, and deformation of the rock between such sliding surfaces is below the limit of detection. There are two different sliding mechanisms which are distinguishable in the field.

(*a*) *Stress criterion for frictional sliding*

Many workers assume outright that the slip associated with thrusting obeys the linear law of sliding friction between solids (e.g. Hubbert & Rubey 1959; Carlisle 1965; Hsu 1969). This type of sliding law states that slip cannot occur unless the shearing stress τ_n along the sliding surface reaches a certain value determined by the coefficient of sliding friction μ, the normal stress on the sliding surface σ_n, and the ratio λ of pore pressure to normal stress on the surface:

$$\tau_n = \tau' + \mu(1-\lambda)\,\sigma_n. \tag{20}$$

Here τ' is a constant shear stress below which sliding cannot occur even with $\sigma_n = 0$ or $\lambda = 1$.

By considering the details of the physical processes which operate along the sliding surface it is possible to derive this sliding law from first principles. For example, asperities project from one surface towards the other (figure 8*a*). These asperities slide along, indenting and penetrating, and eventually break off producing wear particles. Assuming that the asperities break off in a brittle-elastic fashion when their finite shear fracture strength is reached, Byerlee (1967) was able to derive the linear frictional sliding law (equation (20)).

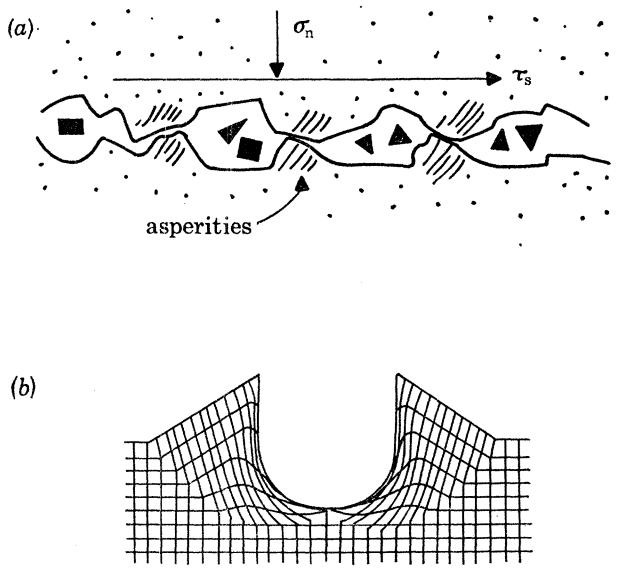

FIGURE 8. (*a*) Longitudinal section through a sliding surface undergoing shear and normal stresses τ_s, σ_n. Behaviour of the asperities is the key to deriving the linear sliding criteria by either brittle-elastic fracturing or plastic yielding. Black wear particles (tectonic breccia) are accumulating.

(*b*) Cross section through such a sliding surface showing the plastic deformed zone on both sides of a track left by a rigid asperity. Compare with figure 13*c*.

This linear sliding law can also be derived if the microscopic processes involve perfectly plastic yielding rather than elastic-brittle fracturing. In this case the asperities plough through the surface as a cutting or scratching process (figure 8*b*), forming junctions or welds which are then sheared off by plastic yielding (Bowden & Tabor 1964).

These physical mechanisms produce diagnostic minor features on the sliding surfaces. For example, figures 9, 10 and 11, demonstrate a sliding surface which has an observed magnitude and sense of slip. This surface shows striations, raised steps, chevron marks, flutes, and crescentic gouge marks (Wegmann & Schaer 1957; Dzulynski & Kotlarczyk 1965; Tjia 1968). These minor structures may be used as a guide to the processes going on, and whenever a particular sliding surface is covered by this type of feature the linear frictional sliding criteria was in force. These sliding surface markings are virtually identical to some of those formed beneath glaciers; they must be produced in the same way and I see no reason for a distinct terminology.

(*b*) *Pressure solution slip*

Many of the sliding surfaces in the central Appalachians are covered by 'fibrous mineral growth' (Cloos 1971, p. 52), often arranged into imbricated 'fibrous shingles' or 'accretion steps' (figure 13). These fibre coated sliding surfaces have also been recognized in the Western Alps (Durney & Ramsay 1973), and they are widespread in the Canadian Rockies (figures 11,

12, 14, 15). Striations and grooves are also found, produced by pressure solution around resistant and sliding tools (figure 13*c*). All scales of styolites abound in the wall rock around the slip surfaces.

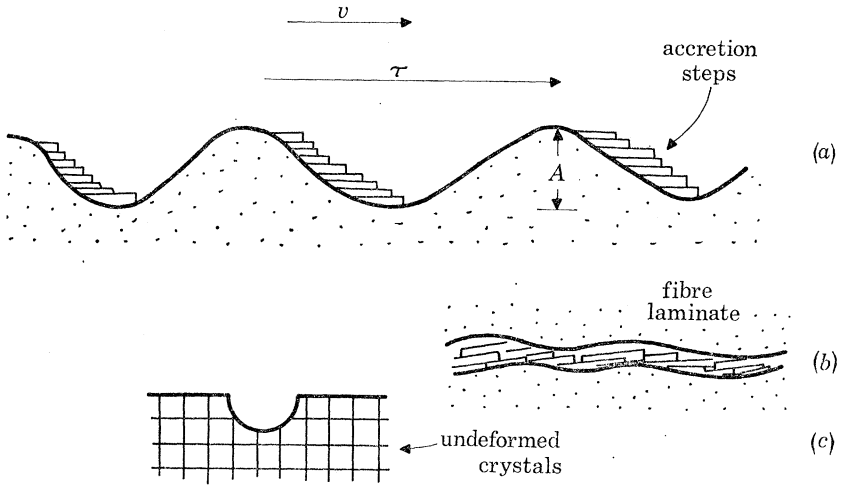

FIGURE 13. (*a*) Longitudinal section through a sinusoidal surface with amplitude A undergoing pressure solution slip with velocity v under a shear stress τ_n. Accretion steps produced on lee side of bumps. If fibres terminate with euhedral crystal faces and into vuggy fillings, this is evidence of a fluid-filled void and these are occasionally found on the lee side of accretion steps.

(*b*) Fibres between two sliding surfaces build up into a 'fibre laminate', in which fibres form thin layers, often with different orientation, grain size, and composition in each layer.

(*c*) Cross section through a groove left by a tool which has presolved its way across surface. Crystals adjacent to groove are essentially undeformed (compare with figure 8*b*).

Such sliding surfaces, covered with fibres, grooves, and accretion steps, are promptly pronounced to be 'slickensided' by most geologists who see them. Unfortunately the term slickenside often has genetic connotations of abrasive scratching produced by sliding friction (equation (20)). I will use slickenside in a purely descriptive and non-genetic fashion in this article.

It has been shown elsewhere that pressure solution and fibrous growth are diagnostic of diffusion creep, for which an explicit flow law may be written (Elliott 1973). We shall now show that a diffusion controlled *sliding law* may be inferred from a slip surface covered with fibre growth and pressure solution features.

An ideal surface exactly planar down to an atomic scale could slide without the necessity of transport of material along the surface. There is, of course, no such thing as a perfectly smooth surface and, with protrusions, sliding is possibly only if material is transported from one part of the surface to another. One way of moving such material about is by diffusion from the stressed surface, into the diffusion 'pipe', and precipitation on a less stressed part of the surface. Define a 'metamorphic quantity' M,

$$M = \Omega\delta D/kT. \tag{21}$$

The diffusion coefficient D at absolute temperature T is that of the rate limiting ionic species with atomic volume Ω travelling in a grain boundary or solution film of thickness δ (see Elliott (1973) for further discussion of these quantities and Fisher & Elliott (1974, Fig. 2), for possible values of D). This metamorphic quantity M has the dimensions of volume flow rate of material per unit shear stress. At a given shear stress a large flow of material (a high value of M) would allow a high rate of sliding.

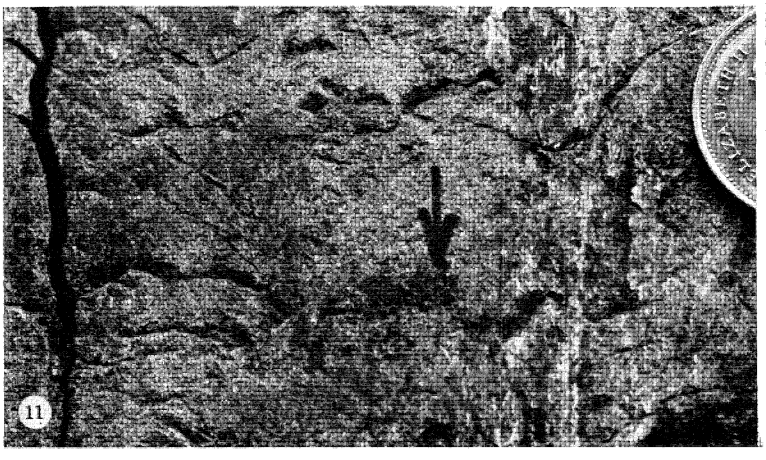

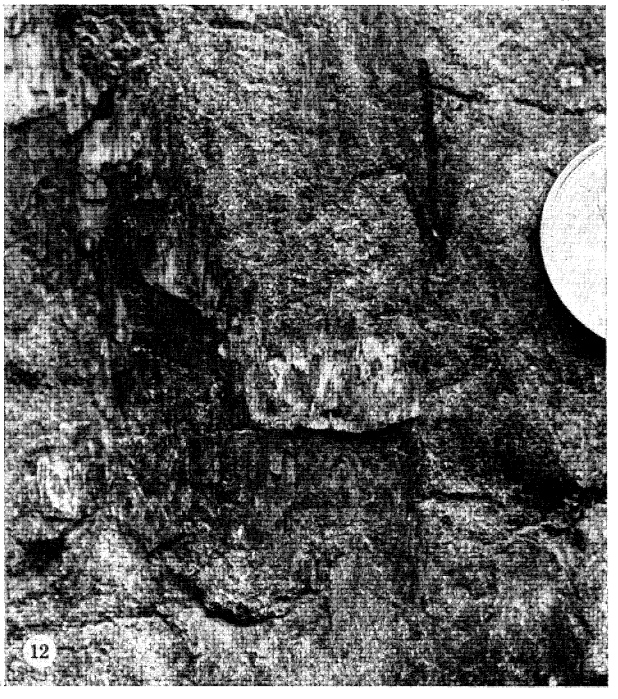

FIGURE 9. Minor contraction fault. On the exposed right face are a number of sliding features which indicate the physics of the sliding process. In photos (figures 10, 11 and 12) of these sliding features arrows indicate downward slip of the left side over this exposed right face. Scale is 1 m, note that displacement on the fault is a few metres. Upper Cretaceous Brazeau formation along Sheep Creek in the Panther Culmination (figure 4). Thickness of overburden $\approx$ 5 km.

FIGURE 10. Stepped surface with steps facing opposite sense of motion of left side of fault. Frictional sliding; a tool might have burst, leaving a step (Lindström 1974), or it may be a Hertzian crack.

FIGURE 11. Tectonic chevron marks, horns point in sense of motion of left side of fault. Caused by frictional sliding of indentor which is not rolling, Hertzian cone cracks form behind this tool (MacClintock 1953): note fibre between coin and arrow.

FIGURE 12. Fibrous quartz in accretion steps facing in the sense of motion of left side of fault. Evidence of pressure solution slip such as this covers far less surface area at this outcrop than minor features produced by frictional sliding.

(*Facing p.* 306)

PHILOSOPHICAL TRANSACTIONS OF THE ROYAL SOCIETY A MATHEMATICAL, PHYSICAL & ENGINEERING SCIENCES

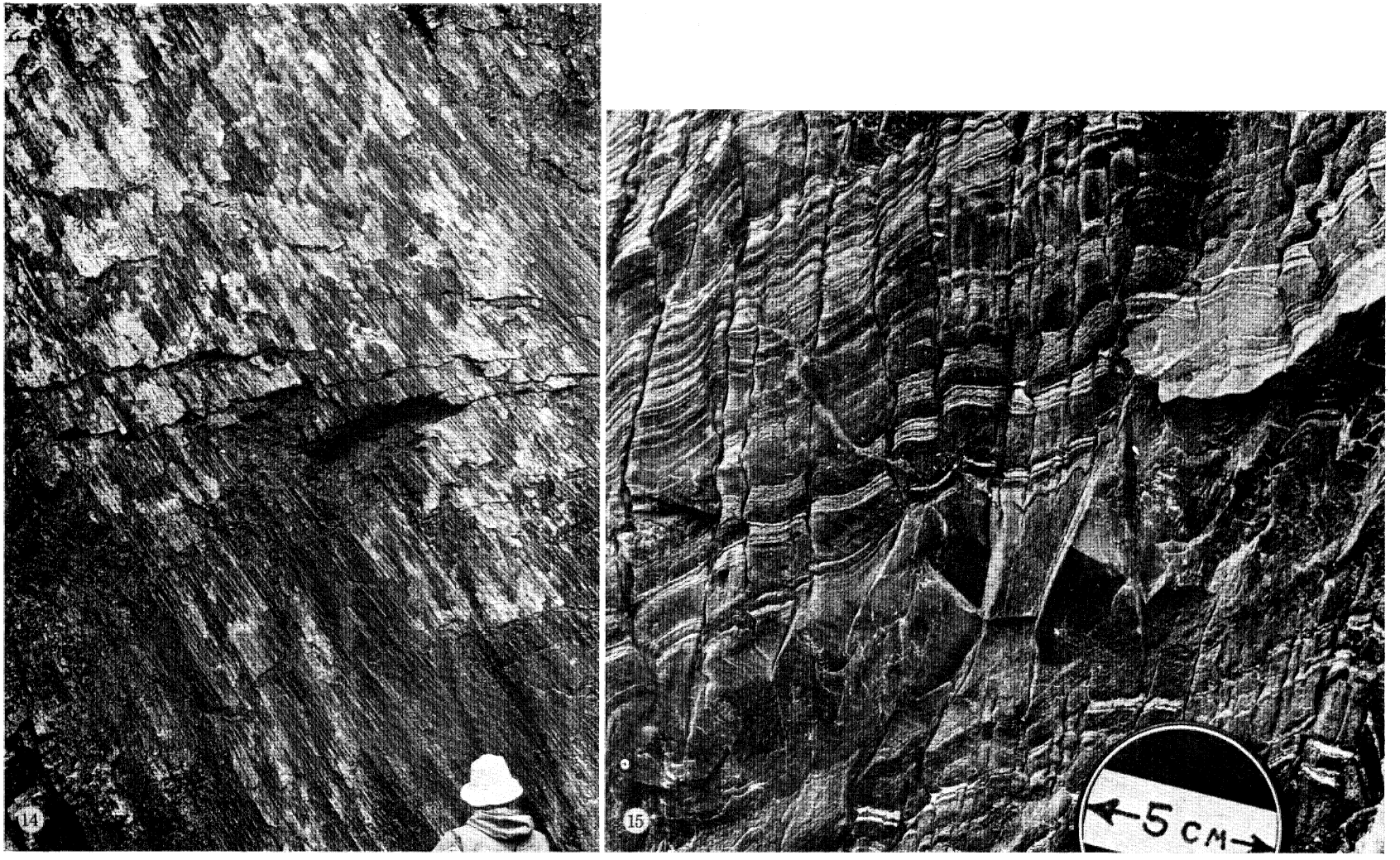

FIGURE 14. Fibrous accretion steps on fault surface in Cambrian carbonates of Mid-Chancellor formation 0.8 km west of Field on Trans-Canada Highway. Rocks are also intensely cleaved by pressure solution processes. Overburden $\simeq$ 8 km.

FIGURE 15. Thin light layers are made up of vertically oriented fibrous growth between beds which are drifting apart. Intense pressure solution cuts beds and also is affecting previously deposited fibres, recycling them. Penetrative pressure solution is the dominant deformation process at this outcrop, which is near that of figure 14.

It is possible that much of the diffusion along sliding surfaces occurs in a discrete, hydrous film rather than by grain boundary diffusion. Evidence of open spaces and a hydrous film are fibre terminations with euhedral crystal faces and open-space drusy fillings behind bumps and accretion steps.

Approximate a sliding surface by a sinusoidal one with amplitude A (figure 13*a*). It can be shown that if a shear stress τ is applied parallel to the surface an exact solution for the velocity (after Raj & Ashby 1971),

$$v = (8M/\pi A^2)\tau. \tag{22}$$

It is interesting that the wavelength does not appear in this equation. A sinusoidal surface is a convenient approximation for any clearly periodic bumps and differs by not more than a factor of two from more exact solutions. Diffusional redistribution quickly removes local irregularities and reveals the basic periodic pattern.

(*c*) *Relative importance of the discrete sliding mechanisms*

We have two processes of slip on discrete surfaces: frictional sliding (equation (20)) and pressure solution slip (equation (22)). Each of these processes does not need to wait for the other to happen; they can occur either simultaneously or in any time order. In other words frictional sliding and pressure solution slip are *independent* processes. If a sliding surface is entirely covered by fibrous growth and pressure solution features the sliding mechanism is essentially pressure solution slip, and in a similar way we can identify frictional sliding. Most sliding surfaces I have observed are clearly in one category or the other, but the mixed case could be handled by assuming that the ratio of frictional to pressure solution slip is equal to the ratio of surface areas covered by pressure solution versus frictional sliding features. For example, at the Sheep Creek locality (figures 9, 10, 11 and 12) frictional sliding features cover a far higher percentage (*ca.* 80) of the observed surface area than do pressure solution features. The work W by either frictional or pressure solution sliding of m such sliding surfaces of a particular type in a volume of rock is

$$W = \sum_{0}^{m} u_m \tau_m S_m \tag{23}$$

where u_m, τ_m is the displacement and shear stress on the mth surface whose surface area S_m is covered by minor structures of a particular type.

Whole rock deformation

Rather than being restricted to a discrete surface, slip may be distributed over an intensely deformed layer of finite thickness bounded by zones of much less deformed material. These zones of whole rock deformation range in thickness up to thick zones of penetrative whole rock deformation with strain gradients extending over several kilometres.

(*a*) *Thin deformation zones*

These are low grade versions of the ductile shear zones described by Ramsay & Graham (1971) from high grade rocks. There are three different ways for these thin (< 100 m) deformation zones to originate.

PHILOSOPHICAL TRANSACTIONS OF THE ROYAL SOCIETY A MATHEMATICAL, PHYSICAL & ENGINEERING SCIENCES

(i) *Perfectly rough surfaces*

It is possible that the asperities interlock to such an extent that the surfaces can be described as 'perfectly rough' and the wall rock on both sides deforms as a mass. This could arise along sliding surfaces if the pore pressure became sufficiently low. Clearly the concept of sliding friction is no longer useful when we reach 'full' or 'sticking' friction, as it is known in plasticity. Pressure solution slip could also get locked up in a similar fashion. These cases are recognized. In the field they appear as discrete surfaces with a definite but small amount of slip compared to the displacement accounted for the ductile shear zones with continuous strain gradients in the adjacent wall rock; and they are occasionally identified as 'feather' or 'pinate' joints or gash veins.

(ii) *Tectonic breccia*

After a certain amount of frictional sliding along discrete surfaces, wear particles accumulate into a continuous layer of breccia separating the two moving surfaces. Within this tectonic breccia the strain is accomplished by ductile deformation in the particles and sliding of the particles over each other accompanied by progressive reduction in size. The deformation may be distributed throughout this deformation zone and the finite strain recorded by such breccia could be enormous.

Such granular aggregates have been extensively studied in soil mechanics. In bulk, the breccia may be described as an ideally plastic solid with a Mohr–Coulomb yield surface,

$$\tau_y = \tau^0 + \tan\phi(1-\lambda)\,\sigma_n. \tag{24}$$

Here σ_n is the normal stress on the boundaries of the deformation zone and the slope ϕ of the yield envelope is determined from a Mohr diagram. τ^0 is a constant.

This breccia is frequently observed. Even major thrust surfaces may have a layer of tectonic breccia only a few centimetres thick, although there are a few reports of breccia layers along thrusts which are as thick as 20 m (Stanley & Morse 1974). But tectonic breccia does not appear to cover the majority of sliding surfaces within the body of the thrust sheet.

(iii) *Shale, coal, evaporites, serpentinite*

These easily deformed rocks cover a substantial percentage of the surface area of many thrust faults. Such rocks could even be produced by the thrust motion itself, by breaking down the tectonic breccia to clay size particles as suggested by Wilson (1970) and Engelder (1974). Serpentinite and gypsum could have a high pore pressure effect (λ near 1) as a result of dehydration reactions (Raleigh & Patterson 1965; Heard & Rubey 1966). Again, an ideally plastic solid with Mohr–Coulomb yield surface (equation (14)) is favoured.

It is interesting that two of the equations discussed above are *formally* identical but have quite different *physical* interpretations; this has produced some confused discussion. The first equation (20) is a stress condition for frictional sliding of two surfaces in direct contact. The second equation (24) is a plastic yield condition for a finite volume of material, which could be (1) the deforming wall rock, (2) tectonic breccia, or (3) shale, coal, evaporites or serpentinite.

Special and rather unique rock types such as shale, coal, gypsum, and serpentinite cannot provide a general solution, for although all of these rocks can be found along various thrust surfaces, much of the energy involved in the emplacement of a thrust sheet may be dissipated

within the main mass itself rather than by basal slip. Recall also that thrusts become more difficult to create and propagate (W_e and W_p) in ductile rocks. Such rocks tend to deform and flow rather than fracture.

(*b*) *Regional penetrative deformation*

Penetratively deformed rocks are immediately recognized by throughgoing metamorphic fabrics such as cleavage and stretching direction. Finite strains are large, and strain gradients occur over distances of the order of kilometres. We must use the constitutive equations appropriate for a three dimensional volume. Flow laws relating stress to strain rate depend exponentially upon temperature and on an inverse power of the grain size.

In low grade rocks pressure solution (or grain boundary diffusion) creep is often the dominant process,

$$\dot{\gamma} = (1/\eta)\tau.$$

Grain boundary diffusion creep is a Newtonian flow with viscosity η,

$$\eta = d^3 r^{\frac{3}{2}}/K'\pi M.$$

In this equation d is grain diameter, r is grain axial ratio, and K' is a constant which may have a value between 21 and 8γ (Elliott, 1973).

Many of the formations in the Western Main Ranges show a penetrative cleavage (Cook 1975). This cleavage is of pressure solution type – indicating Newtonian flow (figure 15).

The rate with which deformation work is expended per unit volume in a simple shear path with steady flow is

$$\dot{\omega} = \tfrac{1}{2}\tau\dot{\gamma} = \left(\frac{\eta}{2}\right)\dot{\gamma}^2,$$

therefore

$$W = \left(\frac{\eta}{2t^2}\right)\gamma^2.$$

We see that deformation work depends upon a *power* of the finite shear strain.

At higher temperatures and coarse grain sizes dislocation creep is important, with the shear strain rate $\dot{\gamma}$ dependent upon the shear stress τ to some power n,

$$\dot{\gamma} \propto \tau^n.$$

The work W due to each of the whole rock deformation mechanisms, such as pressure solution and dislocation creep, must be separately evaluated.

Which were the main energy dissipating processes within the mass of the thrust sheet? Information from several sources can be patched together onto a cross section of the McConnell thrust (figure 16).

(1) In the Central Appalachians penetrative cleavage and finite strain – almost entirely a result of massive pressure solution – is observed to become a dominant process when the metamorphic temperatures reach $\geq$ 250 °C (Elliott 1973, and in preparation). With a thermal gradient between 25 °C km^{-1} and 50 °C km^{-1} this temperature would be reached at depths between 9.2 and 4.6 km. The 250° isotherm is sketched onto the cross section (figure 16).

(2) The overburden during deformation of the outcrops illustrated in this paper can be estimated (figure 16). Processes observed in these outcrops are related to adjacent thrusts, but they can be placed in the structural positions they might occupy if they had deformed within the moving McConnell thrust mass.

We find that as the depth of overburden increases (and metamorphic temperature) there is a transition from frictional sliding to pressure solution slip, but that shortly after the zone of extensive pressure solution slip is reached the rock becomes penetratively cleaved (figure 15). About half the volume of the McConnell thrust system is stamped with this penetrative pressure solution cleavage, and much of the finite strain within the thrust system occurred here.

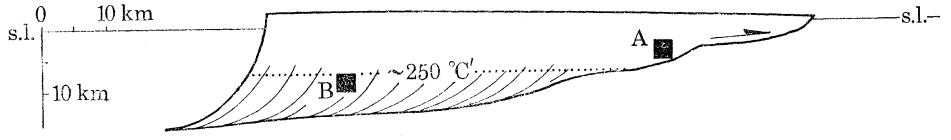

FIGURE 16. Outcrops associated with different thrusts may be interpreted as if they were at corresponding geological positions within the same thrust sheet. In this case A represents the outcrop of figures 9, 10, 11 and 12 and B the outcrops of figures 14 and 15. The position of the 250 °C isotherm is sketched in.

CONCLUSIONS

Knowing the initial and final geometry of the thrust fault system it is possible to calculate the gravitational work involved in thrusting. For the entire McConnell thrust sheet, gravity spreading is the appropriate theory because the gravitational work of 7.3×10^{19} J is much greater than the maximum possible work by any surface forces. But if one considers smaller portions of the McConnell, longitudinal compressive surface forces are important. For example if one considers only the major imbricate slice negligible gravitational work is accomplished; on a still smaller scale the front toe portion has its centre of gravity raised and gravity is a resisting rather than a driving force.

A new theory for the initiation and growth of thrust fault surfaces is outlined. It is found that the maximum displacement along thrusts is linearly related to their map length. Fold complexes at the lateral ends of thrusts appear roughly constant in size for a given metamorphic grade. These observations suggest that thrust fault surfaces are formed as ductile fractures, and the theory predicts increasing difficulty in forming thrusts as the ductility rises, such as would be produced by increase in metamorphic grade. Whenever thrust displacement is greater than a few kilometres, then the work involved in basal sliding is larger than that required to propagate the thrust.

Finite simple shear within the body of the sheet is necessarily transferred into displacement along the thrust fault surface wherever the thrust cuts up section in the hanging wall. Bending the thrust over obstacles in the footwall sets up simple shear and flexural slip folding within the body of the sheet. A substantial amount of work is expended in this internal deformation, and even for major thrusts like the McConnell this work of internal deformation may exceed that of basal sliding.

This picture of the growth of thrust faults can be checked by field work, and it is also possible to establish the physical mechanisms of rock deformation by field observations. A novel type of sliding along discrete surfaces is pressure solution slip, in which obstacles are bypassed by diffusive mass transfer. Fibres and pressure solution grooves are diagnostic features of this sliding law, in which the velocity of sliding is linearly related to the applied shear stress. It appears that roughly a 5 km thick surface layer of the McConnell thrust system was dominated by linear frictional sliding. Pressure solution slip only becomes significant deeper than about 5 km, but at this depth penetrative whole rock deformation – marked by cleavage and stretching directions –

is becoming dominant with regional strain gradients of the order of kilometres. This penetrative whole rock deformation occupies roughly half the volume of the McConnell thrust system, and accounts for most of the finite strain and deformation work. Pressure solution is the most important kind of whole rock deformation, suggesting that the McConnell thrust has a frictional sliding surface layer overlying a massive linearly viscous core.

The National Science Foundation supported the work reported in both this and a companion paper (Elliott 1976*a*) on thrust faults. My colleagues and students at Johns Hopkins criticized this paper and suggested several improvements. The Geological Survey of Canada provided both an office in Calgary and incisive discussion.

References (Elliott)

Bally, A. W., Gordy, P. L. & Stewart, G. A. 1966 Structure, seismic data, and orogenic evolution of southern Canadian Rocky Mountains. *Bull. Can. Petrol. Geol.* **14**, 337–381.

Barnes, W. C. 1966 Mechanics of overthrust faulting. *Abstract Geol. Soc. Am. Mtg.*

Batchelor, G. K. 1965 *An introduction to fluid dynamics*. Cambridge University Press.

Bowden, F. P. & Tabor, D. 1964 *The friction and lubrication of solids* Vol. 2. Oxford University Press.

Byerlee, J. D. 1967 Theory of friction based on brittle fracture. *J. Appl. Phys.* **38**, 2928–2934.

Carlisle, D. 1965 Sliding friction and overthrust faulting. *J. Geol.* **73**, 271–291.

Carrigy, M. A. 1971 Lithostratigraphy of the uppermost Cretaceous (Lance) and Palaeocene strata of the Alberta plains. *Res. Council Alberta, Bull.* **27**.

Cloos, E. 1971 *Microtectonics along the western edge of the Blue Ridge, Maryland and Virginia*. Baltimore: The Johns Hopkins Press.

Cook, D. G. 1975 Structural style influenced by lithofacies, Rocky Mountain Main Ranges, Alberta–British Columbia. *Geol. Survey Can. Bull.* **233**, 73 p.

Dahlstrom, C. D. A. 1970 Structural geology in the eastern margin of the Canadian Rocky Mountains. *Bull. Can. Petrol. Geol.* **18**, 332–406.

Douglas, R. J. W. 1958 Mount head map-area, Alberta. *Geol. Surv. Can. Mem.* **291**, 241 pp.

Durney, D. W. & Ramsay, J. G. 1973 Incremented strains measured by syntectonic crystal growths. In *Gravity and tectonics* (ed. A. D. Kees & R. Scholten). New York: John Wiley and Sons.

Dzulynski, S. & Kotlarczyk, J. 1965 Tectoglyphs on slickensided surfaces. *Bull. Acad. Polonaise Sci. Géolog.* **13**, 149–154.

Eisbacher, G. H., Carrigy, M. A. & Campbell, R. B. 1974 Paleodrainage pattern and Late Orogoenic basins of the Canadian Cordillera. *Tectonics and sedimentation* (ed. W. R. Dickinson). Soc. Econ. Paleo. and Min., Special Pub. 22, 143–166.

Elliott, D. 1972 Deformation paths in structural geology. *Geol. Soc. Am. Bull.* **83**, 2621–2635.

Elliott, D. 1973 Diffusion flow laws in metamorphic rocks. *Geol. Soc. Am. Bull.* **84**, 2645–2664.

Elliott, D. 1976*a* The motion of thrust sheets. *J. geophys. Res., Red.* **81**, 949–963.

Elliott, D. 1976*b* Thrust length, displacement, and breeding behaviour. In preparation.

Engelder, J. T. 1974 Cataclasis and the generation of fault gouge. *Bull. Geol. Soc. Am.* **85**, 1515–1522.

Fisher, G. W. & Elliott, D. 1974 Criteria for quasi-steady diffusion and local equilibrium in metamorphism. In *Geochemical transport and kinetics* (ed. A. W. Hofmann, B. J. Giletti, H. S. Yoder & R. A. Yund). Washington: Carnegie Inst.

Goguel, J. 1948 (2nd edn) Introduction a l'étude méchanique des déformations de l'écorce terrestre. *Mém. Carte Geol. France.* 530 pp.

Heard, H. C. & Rubey, W. R. 1966 Tectonic implications of gypsum dehydration. *Bull. Geol. Soc. Am.* **77**, 741–760.

Heim, A. 1921 Geologie der Schweiz. II. Die Schweizer Alpen. Tauchnitz, Leipzig.

Hsü, K. J. 1969 Role of cohesive strength in the mechanics of overthrust faulting and land sliding. *Geol. Soc. Am. Bull.* **80**, 927–952.

Hubbert, M. K. & Rubey, W. W. 1959 Role of fluid pressure in mechanics of overthrust faulting. *Bull. Geol. Soc. Am.* **70**, 115–166.

Lindström, M. 1974 Steps facing against the slip direction, a model. *Geol. Mag.* **111**, 71–74.

MacClintock, P. 1953 Crescentic crack, crescentic gouge, friction crack, and glacier movement. *J. Geol.* **51**, 186.

PHILOSOPHICAL TRANSACTIONS OF THE ROYAL SOCIETY A MATHEMATICAL, PHYSICAL & ENGINEERING SCIENCES

McClintock, F. A. & Argon, A. S. 1966 *Mechanical behavior of materials*. Reading, Massachussetts: Addison-Wesley.

Nason, R. & Weertman, J. 1973 A dislocation theory analysis of fault creep events. *J. geophys Res., Red* **78**, 7745–7751.

Odé, H. 1960 Faulting as a velocity discontinuity in plastic deformation. In Griggs, D. & Handin, J. (editors), *Geol. Soc. Am. Mem.* **79**, 293–321.

Oldham, R. C. 1921 Know your faults. *Q. J. Geol. Soc. Lond.* **78**, 78–92.

Ollerenshaw, N. C. 1968 Preliminary account of the geology of limestone mountain map-area, southern foothills, Alberta. *Geol. Surv. Can. Pap.* 68–24, 37 pp.

Price, R. A. 1973 The mechanical paradox of large overthrusts. *Abstract Geol. Soc. Am. Ann. Mtg.*

Price, R. A. 1974 Large scale gravitational flow of supracrustal rocks southern Canadian Rockies. In *Gravity and tectonics* (ed. A. J. Kees & R. Scholten). New York: John Wiley and Sons.

Price, R. A. & Mountjoy, E. W. 1970 Geologic structure of the Canadian Rocky Mountains between Bow and Athabasca rivers – a progress report. *Geol. Ass. Can., Spec. Pap.* **6**, 7–25.

Raj, R. & Ashby, M. F. 1971 On grain boundary sliding and diffusional creep. *Metallurg. Trans.* **2**, 1113–1127.

Raleigh, C. B. & Patterson, M. S. 1965 Experimental deformation of serpentinite and its tectonic implications. *J. Geophys. Res. Red* **70**, 3965–3985.

Ramsay, J. G. & Graham, R. H. 1970 Strain variation in shear belts. *Can. J. Earth Sci.* **7**, 786–813.

Stanley, R. S. & Morse, J. D. 1974 Fault zone characteristics of two well exposed overthrusts: the Muddy Mountain Thrust, Nevada, and the Champlain Thrust at Burlington, Vermont. Abstracts NE Sect. *Geol. Soc. Am. Ann. Mtg.*

Tjia, H. D. 1968 Fault-plane markings. 23*rd Int. Geol. Congress* **13**, 279–284.

Wegmann, E. & Schaer, J. P. 1957 Lunules tectoniques et traces de mouvements dans les plis du Jura. *Eclogae Geologicae Helvetiae*, **50**, 492–496.

Wilson, R. C. 1970 Mechanical properties of the shear zone of the Lewis overthrust, Glacier National Park, Montana. Ph.D. Thesis, Texas A and M, 89 p.

PHILOSOPHICAL TRANSACTIONS OF THE ROYAL SOCIETY A MATHEMATICAL, PHYSICAL & ENGINEERING SCIENCES

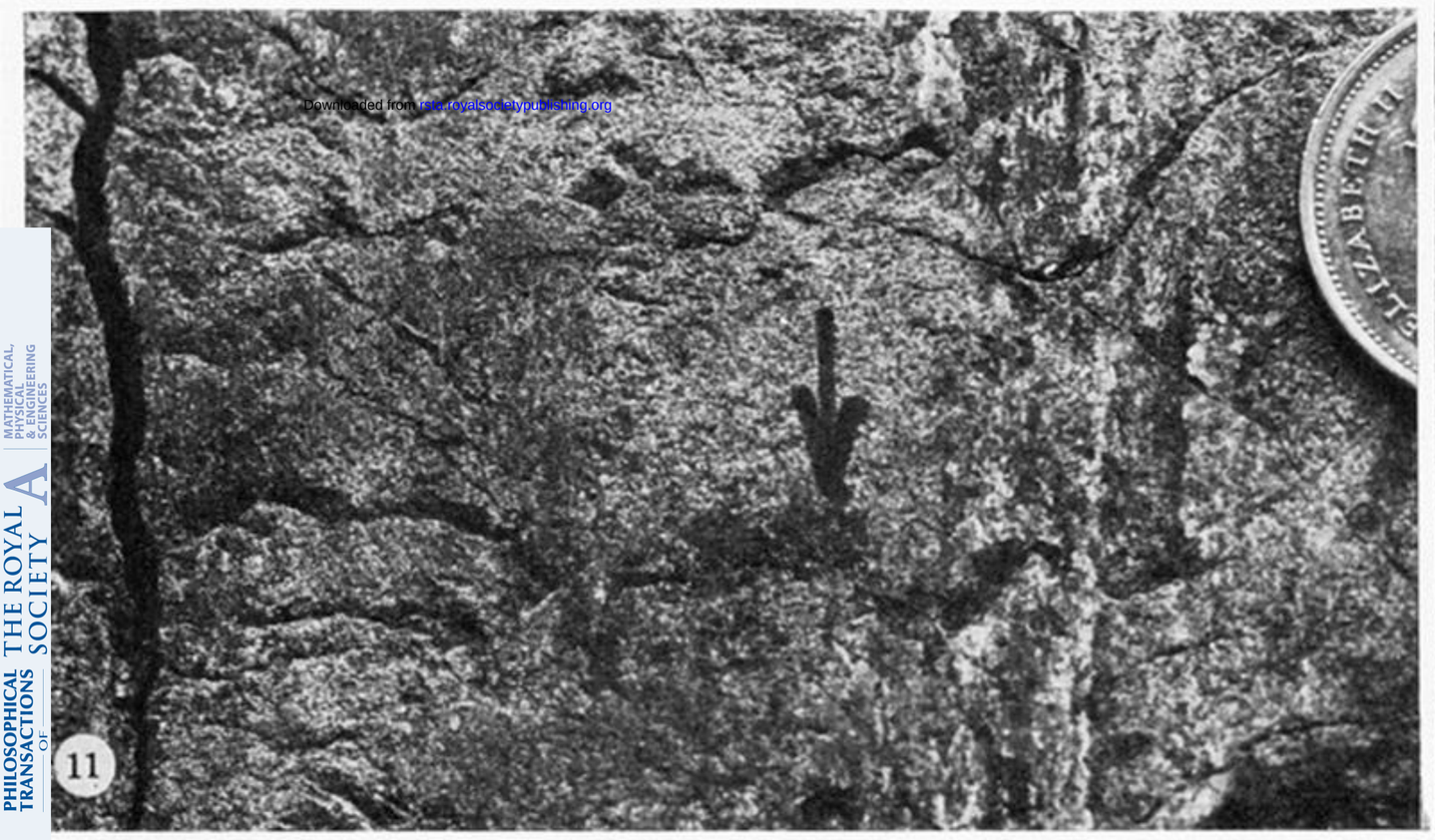

PHILOSOPHICAL TRANSACTIONS OF THE ROYAL SOCIETY A MATHEMATICAL, PHYSICAL & ENGINEERING SCIENCES

FIGURE 9. Minor contraction fault. On the exposed right face are a number of sliding features which indicate the physics of the sliding process. In photos (figures 10, 11 and 12) of these sliding features arrows indicate downward slip of the left side over this exposed right face. Scale is 1 m, note that displacement on the fault is a few metres. Upper Cretaceous Brazeau formation along Sheep Creek in the Panther Culmination (figure 4). Thickness of overburden $\approx$ 5 km.

FIGURE 10. Stepped surface with steps facing opposite sense of motion of left side of fault. Frictional sliding; a tool might have burst, leaving a step (Lindström 1974), or it may be a Hertzian crack.

FIGURE 11. Tectonic chevron marks, horns point in sense of motion of left side of fault. Caused by frictional sliding of indentor which is not rolling, Hertzian cone cracks form behind this tool (MacClintock 1953): note fibre between coin and arrow.

FIGURE 12. Fibrous quartz in accretion steps facing in the sense of motion of left side of fault. Evidence of pressure solution slip such as this covers far less surface area at this outcrop than minor features produced by frictional sliding.

PHILOSOPHICAL TRANSACTIONS OF THE ROYAL SOCIETY A MATHEMATICAL, PHYSICAL & ENGINEERING SCIENCES

PHILOSOPHICAL TRANSACTIONS OF

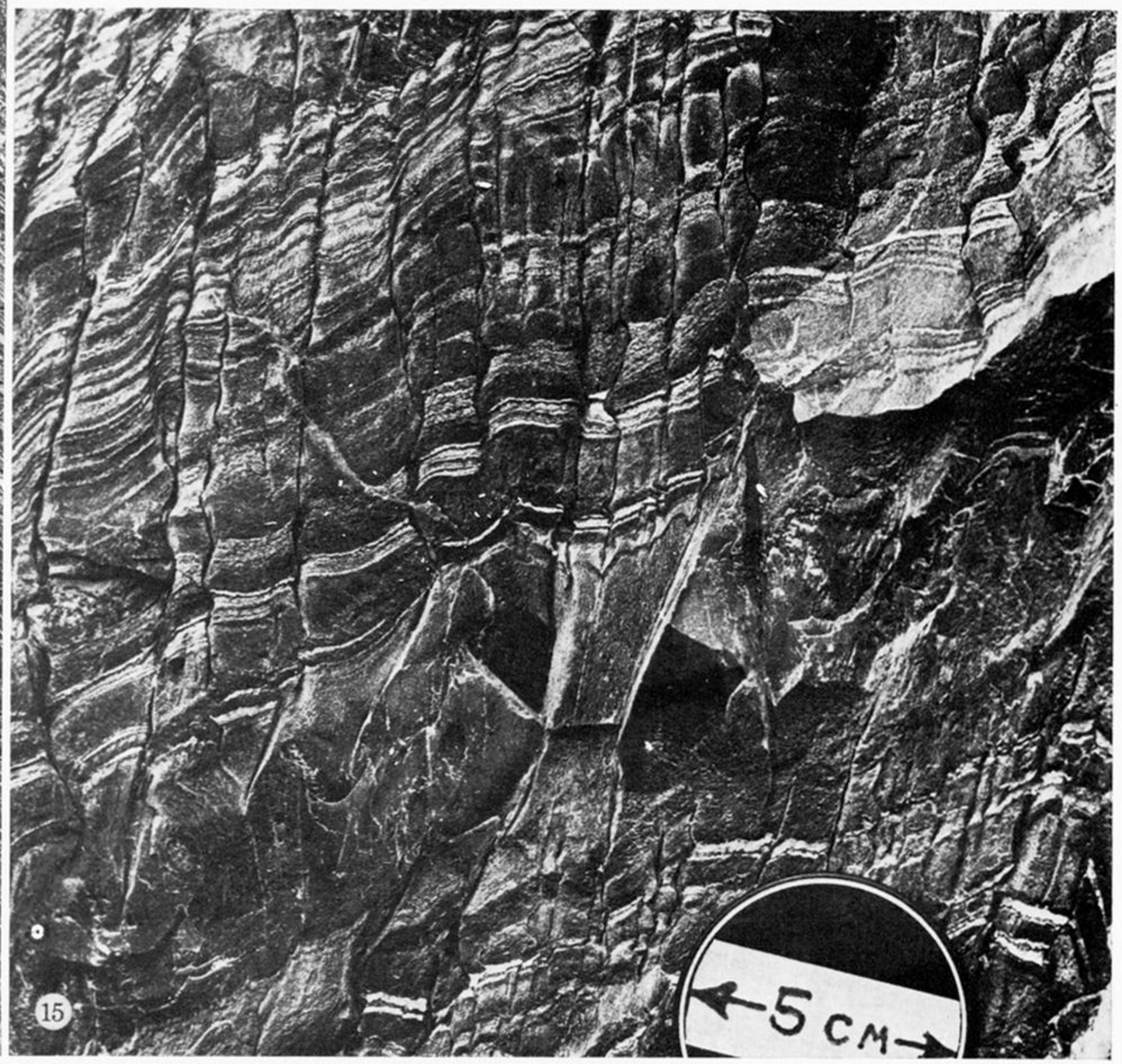

FIGURE 14. Fibrous accretion steps on fault surface in Cambrian carbonates of Mid-Chancellor formation 0.8 km west of Field on Trans-Canada Highway. Rocks are also intensely cleaved by pressure solution processes. Overburden $\simeq$ 8 km.

FIGURE 15. Thin light layers are made up of vertically oriented fibrous growth between beds which are drifting apart. Intense pressure solution cuts beds and also is affecting previously deposited fibres, recycling them. Penetrative pressure solution is the dominant deformation process at this outcrop, which is near that of figure 14.